

Development of the Femoral Bicondylar Angle in Hominid Bipedalism

S. J. SHEFELBINE,^{1,3} C. TARDIEU,² and D. R. CARTER^{1,3}

¹Biomechanical Engineering Division, Mechanical Engineering Department, Stanford University, Palo Alto, CA, USA

²Laboratoire d'Anatomie Comparée, Muséum National d'Histoire Naturelle, Paris, France

³VA Rehabilitation Research and Development Center, Palo Alto, CA, USA

The bicondylar angle is the angle between the diaphysis of the femur and a line perpendicular to the infracondylar plane. The presence of a femoral bicondylar angle in *Australopithecus afarensis* indicates that these 3.5-million-year-old hominids were bipedal. Many studies have linked the formation of the femoral bicondylar angle with bipedality, but the mechanism for the formation of the angle is poorly understood. Mechanical factors, such as stresses and strains, influence the growth process. In particular, previous studies have demonstrated that hydrostatic compressive stress inhibits growth and ossification, and octahedral shear stress promotes growth and ossification. In this study we implemented these mechanobiological principles in a three-dimensional finite-element model of the distal femur. We applied loading conditions to the model to simulate loading during the single-leg stance phase of bipedal gait. The stresses in the physis of the distal femur that result from bipedal loading conditions promote growth and ossification more on the medial side than on the lateral side of the femur, forming the bicondylar angle. This model explains the presence of the bicondylar angle in hominid bipedalism and also the ontogenetic development of the bicondylar angle in growing children. The mechanobiological relationship between endochondral ossification and mechanical loading provides valuable insight into bone development and morphology. (Bone 30:765–770; 2002) © 2002 by Elsevier Science Inc. All rights reserved.

Key Words: Bicondylar angle; Bipedalism; Endochondral ossification; Distal femur development.

Introduction

The earliest known bipedal human ancestors are the australopithecines from about 4.2 million years ago.^{18,19} The bicondylar angle of the femur of australopithecines is often used as a marker of bipedality, and is therefore an indicator of the human lineage.¹ The bicondylar angle is the angle between an axis through the shaft of the femur and a line perpendicular to the infracondylar plane (Figure 1). In modern humans, this angle ranges from 8°–11°.^{22,29} In australopithecines, this angle is slightly larger, between 12° and 15°, and may be related to the short stature,

Address for correspondence and reprints: Dr. Dennis R. Carter, Biomechanical Engineering Division, Mechanical Engineering Department, Durand Building Room 215, Palo Alto, CA 94305-4038. E-mail: drcarter@stanford.edu

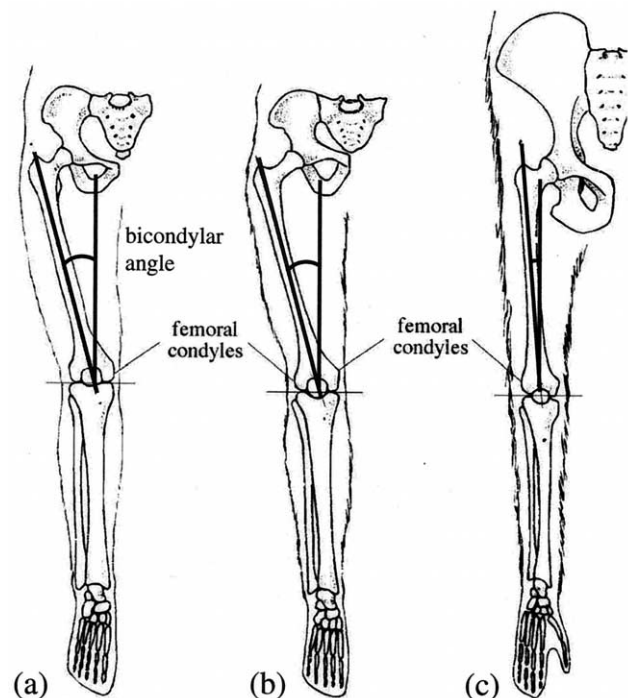


Figure 1. The bicondylar angle in (a) modern humans is 8°–11°, in (b) australopithecines is 14°–15°, and in (c) chimpanzees is 1°–2°. All skeletons have been scaled to the same size for comparison. Reprinted with permission.¹⁶

broad pelvis, and long femoral neck of early hominids.¹¹ In contrast, quadrupedal apes have small bicondylar angles: approximately 5° in orangutans; 1° in chimpanzees; and 2° in gorillas.³⁰ What appears to be a bicondylar angle in some primate femora, particularly orangutans, is the result of a different growth process than that occurring in humans. In orangutans, differential growth occurs in the epiphysis in which the medial condyle becomes superiorinferiorly longer than the lateral condyle. This should not be confused with a bicondylar angle due to metaphyseal growth such as in the human femur.³⁰

The bicondylar angle is a particularly intriguing morphological structure because its development in ontogeny (development of an individual) has significant implications for its appearance in phylogeny (development throughout evolution). Ontogenetically, the bicondylar angle forms while the femur grows in early



Figure 2. Femoral diaphysis with the proximal and distal epiphyses removed. The angle shown is with reference to the metaphyseal growth front. From left to right, the femora are at ages 7 years, 5 years, 3 years, 7 months, and a 7 month fetus. Reprinted with permission.²⁹

childhood. When a child is born, the axis of the shaft is perpendicular to the metaphyseal growth front (**Figure 2**). When a 1-year-old child first starts to walk, the medial side of the distal metaphysis grows faster than the lateral side, resulting in the bicondylar angle. The angle reaches a stable value of 8°–10° by the age of 8 years.²⁹ In bedridden children, children with neuromuscular disorders, and paraplegic children who do not walk during the early stages of childhood development, the bicondylar angle does not form.³¹ Therefore, the formation of the bicondylar angle is clearly an epigenetic phenomenon, in which growth of the distal femur is influenced by the mechanical loading environment. Although there is a clear link between the bicondylar angle and bipedalism, little work has been done to demonstrate the mechanism by which bipedalism results in the bicondylar angle.

Long bones, such as the distal femur, grow in length through the process of endochondral ossification. In this process, cartilage cells proliferate, mature, and hypertrophy (expanding particularly in the longitudinal direction). These distinct stages of cellular differentiation are seen in the columns of cartilage cells that align perpendicularly to the growth front. As the cells hypertrophy and die, the matrix surrounding the cells calcifies, and the cartilage is eventually replaced by well-vascularized bone. This process is regulated by: (1) biological factors, such as hormones, growth factors, and other systemic chemical agents; and (2) mechanical factors, such as joint loading and muscle contractions, which impose stresses and strains on the developing bone. It is these mechanical influences that are the focus of this research.

Mechanobiology is the regulation of biological processes by mechanical factors. Previous studies have proposed that the endochondral ossification process is modulated by stresses and strains in the differentiating cartilage.^{3,7,23,32} In other words, certain loading conditions create stress states that may accelerate or decelerate the rate of endochondral growth and ossification. Pauwels hypothesized that “unequal pressure in the epiphyseal cartilage, provided it is not above a certain threshold, leads to unequal growth in length.”²³ Pauwels reasoned that higher compression on one side of the growth front would accelerate growth until the compression was equal across the growth front. Preuschoft and Tardieu have applied this hypothesis to the phylogenetic appearance of the bicondylar angle in early bipedal hominids.²⁴ This hypothesis explains only the simplified loading case in which the stress is assumed to be uniaxial. In an actual

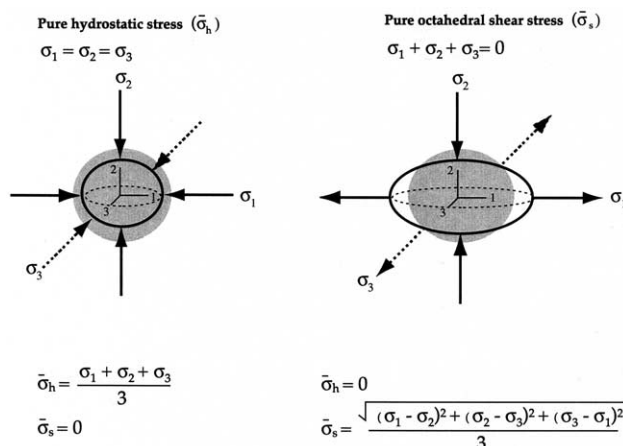


Figure 3. Illustration of the principal stresses (σ_1 , σ_2 , and σ_3) and deformations (solid lines) that are associated with pure hydrostatic stress and pure octahedral shear stress. A general multiaxial stress state will have both hydrostatic and octahedral shear stress components.

joint during bipedal gait, the stresses are complex and multiaxial. Therefore, it is necessary to elaborate on Pauwels’ hypothesis to more general, multiaxial stress conditions.

Previous studies by Carter et al.³ used a multiaxial approach to understand the influence of stresses in endochondral growth and ossification. In this approach the multiaxial stresses are represented by the scalar stress invariants, hydrostatic stress and octahedral shear stress. Stress invariants are independent of reference frame and are therefore useful in describing multiaxial loading conditions. Hydrostatic compressive stress results in a change in volume with no change in shape, if the material is compressible. Octahedral shear stress results in a change in shape with no change in volume (**Figure 3**). In general, a given state of stress will consist of both hydrostatic and octahedral shear stress. It has been proposed that endochondral growth and ossification is inhibited by intermittent hydrostatic compressive stress and accelerated by intermittent octahedral shear stress. This mechanobiological theory has been used to explain and predict the ossification patterns of long bones^{2,3,34} and the sternum,³³ the shapes of the secondary ossific nuclei,⁵ the shape changes that occur at the bone ends during development,¹⁰ the thickness of cartilage in a developed joint,^{4,6,27} and the patterns of degenerative change in the femoral articular cartilage.⁴ Although this theory was used previously to predict locations of bone formation, it can be extended to predict tissue growth and the morphological changes that occur during growth of long bones. The objective of this study is to predict the development of the bicondylar angle by applying these mechanobiological concepts to a three-dimensional finite-element model of the distal femur.

Methods

A finite-element model is a mathematical representation of a structure for which the stresses and strains can be determined at any point within the structure. To determine the effects of stresses during bipedal gait on growth of the distal femur and formation of the bicondylar angle, we developed a three-dimensional (3D) finite-element model of the distal femur.

Model Geometry

A 3D finite-element model was generated to represent a simplified, idealized geometry of the distal femur. The diameter of the

diaphysis was 20 mm, the mediolateral dimension of the epiphysis was 50 mm, and the total length of the model was 100 mm. The dimensions were chosen to represent the distal femur of a 1-year-old child and were confirmed to first approximation using magnetic resonance imaging (MRI) scans of the distal femur of a 2-year-old child. The bicondylar angle was 0° in the initial model.

Model Materials

Each element in a finite-element model has material properties that determine how the material deforms in response to stress. The modulus of elasticity (*E*) is a measure of the stiffness of the material and expresses units of pressure (MPa). A soft material, such as cartilage, has a low modulus of elasticity, whereas a hard material, such as bone, generally has a high modulus of elasticity. Poisson's ratio (*ν*) is a measure of the volume change during compression of a material and can range from 0 to 0.5. A material that has a large volume change, such as porous cancellous bone, has a relatively low Poisson's ratio. The high water content of cartilage, on the other hand, makes it nearly incompressible. Therefore, the volume does not change much under compression, and the Poisson's ratio is 0.49.

All materials in the model were approximated to be single phase, linear elastic, isotropic, and homogeneous. The shaft of the distal femur in the model was composed of newly mineralized cancellous bone with a modulus of elasticity of 500 MPa and a Poisson's ratio of 0.2.⁵ The epiphysis consisted of cartilage elements with a shear modulus of 2 MPa and a Poisson's ratio of 0.49, simulating the near incompressibility of cartilage for loading rates comparable to those experienced during walking.²⁸ The elastic modulus, calculated from the shear modulus and Poisson's ratio, was 6 MPa. The transition zone between the epiphysis and the metaphysis had material properties between those of cartilage and bone (*E* = 50 MPa, *ν* = 0.3) (Figure 4). The region of interest in the model was the cartilage adjacent to the metaphyseal growth front. We assumed the "growth region" to be the five rows of cartilage elements distal to the metaphyseal growth front, representing the cartilage that has started differentiating. The stresses in these elements determined how the growth front progressed.

Loading Conditions

Numerous gait studies and mathematical models have determined the presence of an adducting moment at the knee in adults during walking.^{9,13,14,21,26} The net result of the adduction moment is to move the center of pressure of the knee medially so that more of the load is supported by the medial condyle relative to the lateral condyle. Although few gait studies have been performed on children when they first start walking, it is reasonable to assume that a similar, if not proportionally greater, adduction moment is present in children. During the early stages of bone growth, the medial side of the femur grows more than lateral side at the same time that the neck-shaft angle decreases. Both of these morphological changes move the knee closer to the center of gravity, decreasing the moment about the knee. In addition, supporting structures, such as the tensor fasciae latae, iliotibial tract, and collateral ligaments, develop to resist the adduction moment.

When a child first begins to walk around the age of 1 year, the neck-shaft angle is large (140°),¹⁷ the bicondylar angle is 0°,²⁹ and the knee joint is lateral to the center of gravity (Figure 5). To maintain equilibrium during the single-leg stance phase of gait, there must be a moment, or torque, about the knee. This moment is roughly equal to the body weight multiplied by the lateral

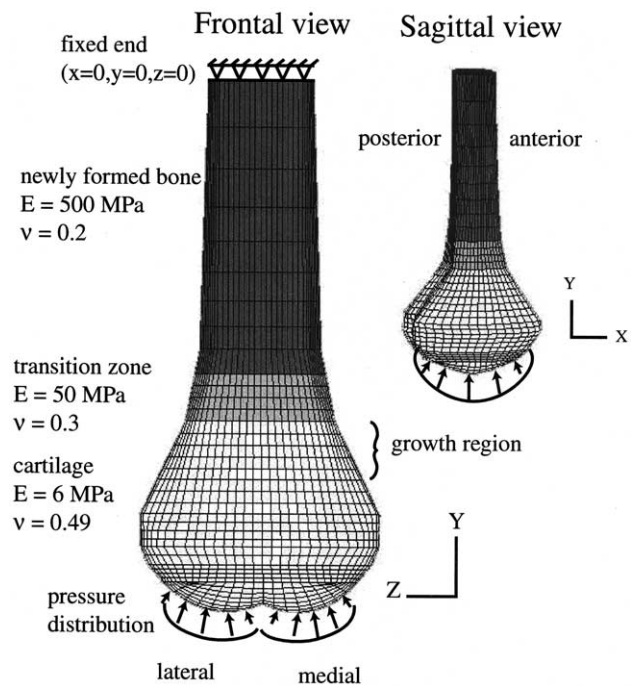


Figure 4. Finite-element model of the distal femur illustrating loading conditions and material properties. The applied pressures are maximum in the center of the condyles and decrease across the condyle. Pressures also decrease anteroposteriorly as shown. The diaphysis of the femur is constrained from moving at the proximal end.

distance to the center of the knee joint. The knee moment is balanced internally by muscle contractions, ligament forces, and asymmetric pressure distributions on the medial and lateral

Bipedal free body diagram (1 year old)

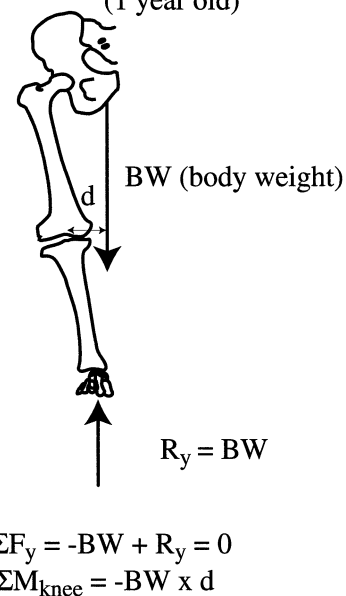


Figure 5. Bipedal gait results in a moment about the knee because the knee is lateral to the center of mass (represented by body weight, BW) in single-leg stance phase of gait. The ground reaction force, *R_y*, is equal to body weight.

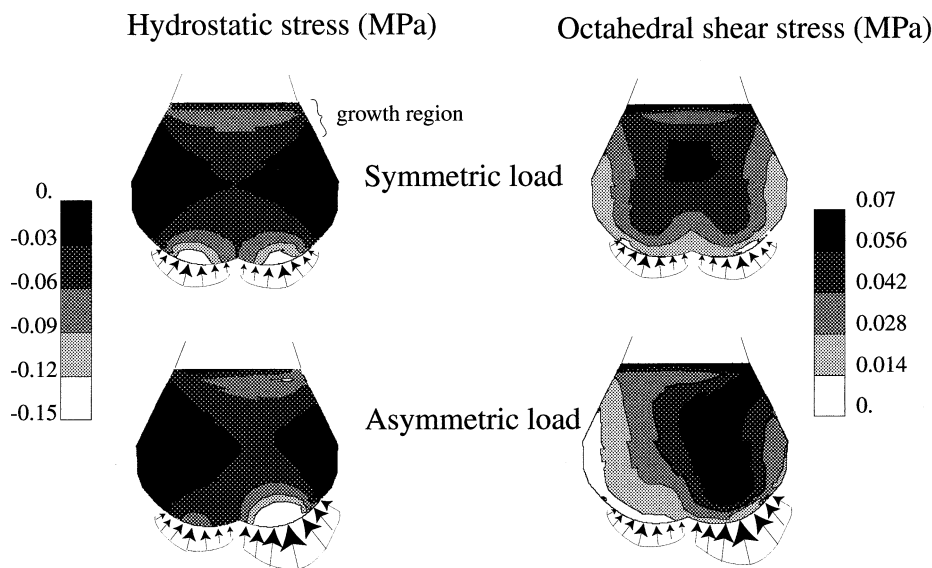


Figure 6. Stress distributions in a coronal slice through the distal femoral cartilage epiphysis. With equal loading on both condyles, the stress distribution is symmetric. When the load on the medial condyle is three times the load on the lateral condyle, the stresses are greater on the medial side of the epiphysis.

condyles. For a first approximation, all moment balancing muscle forces have been lumped together and ligament forces are assumed negligible in this analysis. In contrast to bipeds, most quadrupeds have two feet (usually opposite limbs) on the ground at a time. The center of gravity lies between the two support limbs. This creates a stable structure and there is no moment at the knee in static equilibrium.

Loading on the knee from bipedal gait creates an axial force through the shaft of the femur as well as a moment about the knee. The combination of these loads results in higher loading on the medial condyle relative to the lateral condyle.¹² We applied pressure to the condyles of the finite-element model to simulate loading conditions during bipedal gait. We examined three loading conditions on the condyles of the distal femur. In all cases, the axial force (in the y direction) was 88 N, to represent the body weight of a 1-year-old child. The three loading conditions were: (1) equal pressure on the condyles (no moment); (2) 1.2 times the pressure on the medial condyle relative to the lateral condyle (moment = 76.5 N mm); and (3) 3 times the pressure on the medial condyle relative to the lateral condyle (moment = 383 N mm). In all cases, the pressure was maximum in the middle of the condyle and decreased anteroposteriorly and across the condyle (Figure 4). All loading conditions resulted in <5% maximum principle strain of the cartilage.

Analysis

The specific growth rate ($\dot{\epsilon}$) of a tissue is equivalent to the strain rate (the rate of change in length relative to an initial length). The specific growth rate consists of a baseline biological growth, $\dot{\epsilon}_b$, which is modulated by local mechanical stresses, $\dot{\epsilon}_m$:

$$\dot{\epsilon} = \dot{\epsilon}_b + \dot{\epsilon}_m \quad (1)$$

The biological growth rate represents the growth that occurs due to intrinsic genetic and hormonal regulation. We used a constant value for $\dot{\epsilon}_b$ of 55 $\mu\text{m}/(\text{day} \cdot L_o)$, where L_o is the total length of the growth region. This growth rate is consistent with experimentally determined growth rates in the femoral growth plates of 2-year-olds.¹⁵

The mechanical contribution, $\dot{\epsilon}_m$, can be positive (increasing the total specific growth rate) or negative (decreasing the total

specific growth rate), and is a function of the octahedral shear and hydrostatic compressive stress in the growing tissue:

$$\dot{\epsilon}_m = a\bar{\sigma}_s + b\bar{\sigma}_h \quad (2)$$

Octahedral shear stress, $\bar{\sigma}_s$, is always positive and promotes growth and ossification. Compressive hydrostatic stress, $\bar{\sigma}_h$, is always negative and inhibits growth and ossification. The constants a and b determine the relative amounts that octahedral shear and hydrostatic stress influence growth. We used a ratio of b/a of 0.5 to be consistent with previous studies that have predicted epiphyseal ossification patterns.^{5,34} Magnitudes of $a = 10$ and $b = 5$ were chosen so that the maximum mechanical contribution to growth was less than half the biological growth. Experimental studies on chick embryos have shown that paralyzed limbs, which experience no mechanical stimulation, grow to 50%–60% of the normal length.⁸ It should be noted that this analysis does not depend on the magnitude of the applied load, but rather on the load distribution across the condyles. The constants a and b in Equation 2 can be scaled accordingly to give physiological growth rates that depend on the load magnitude.

From the finite-element analysis we determined the hydrostatic and octahedral shear stresses in the growth region and calculated the total specific growth. The model was then grown using orthonormal expansion of the elements in the longitudinal (y) direction by an amount given by the specific growth rate. We predicted the growth of the femur during a single time interval of 6 months.

Results

A coronal slice through the model illustrates the stress distribution at the center of the cartilaginous epiphysis (Figure 6). With equal loading on the medial and lateral condyles the stress distribution is symmetric. Compressive hydrostatic stress is large at the surface where the load is applied and at the interface with the transition zone. It is the stresses in the growth region adjacent to the transition zone that are of interest because this is the area of cartilage that will calcify next as the growth front progresses. Octahedral shear stress is highest in the center of the epiphysis, which other studies have shown, and predicts the formation of the secondary center of ossification.⁵ Octahedral shear stress is

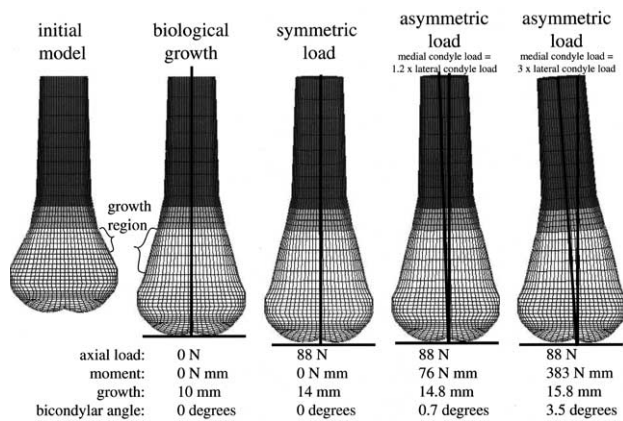


Figure 7. Growth results for the distal femur after 6 months of growth.

slightly higher at the edges of the growth region than in the center. The asymmetric loading stress contours (Figure 6) indicate stress distributions for the case in which the load on the medial condyle is three times the load on the lateral condyle. The hydrostatic and octahedral stresses are much greater on the medial side of the growth region than on the lateral side.

From the calculated stresses, the specific growth rate in the growth region was determined using Equation 1. The growth results predict the bone growth for the different loading conditions (Figure 7). Without loading, the biological component of the specific growth rate, $\dot{\epsilon}_b$, results in equal growth across the growth front and a lengthening of the bone by 10 mm. With symmetric loading on the condyles, the bone grows slightly more to 14 mm. As the load on the medial condyle increases relative to the lateral condyle, the bone grows more on the medial side. The octahedral shear stress promotes growth more than the hydrostatic stress inhibits growth, resulting in asymmetric growth. When the load on the medial condyle is 1.2 times greater than the lateral condyle load, the asymmetric growth resulted in a bicondylar angle of approximately 0.7°. When the medial load was three times the lateral load, the growth was even more asymmetric, resulting in a bicondylar angle of 3.5°.

Discussion

Mechanobiological principles can be used to explain the formation of the bicondylar angle during bipedal gait. Only a small moment at the knee is necessary for the stress distribution in the cartilaginous epiphysis to be asymmetric and result in asymmetric growth across the growth front. With a load 20% greater on the medial condyle, the predicted bicondylar angle was 0.7° after 6 months of growth. Growing at this rate until the age of 8 years, when the bicondylar angle becomes stable, would result in a bicondylar angle of approximately 10°.

This model simplifies the loading conditions on the femur by assuming a single pressure distribution. In vivo, there are many muscles, ligaments, and other structures, such as the patella, that also impose stresses on the developing cartilage. We combined the overall effects of these forces into a single pressure distribution. We chose to examine only the single-leg stance phase of gait, when the loads on the femur are the highest. A more accurate loading scheme would incorporate movement of the tibia over the condyles of the femur during an entire gait cycle. However previous studies have shown that it is the maximum octahedral shear stress and minimum hydrostatic stress in a loading cycle that are likely to have the greatest effect on the endochondral ossification process.²⁷ Therefore, estimating the

gait cycle with a single loading condition is accurate to a first approximation for this application.

This analysis did not account for the presence of the secondary center of ossification in the epiphysis. The secondary center begins to calcify prenatally and expands radially during growth. Although this bony nodule will affect the local stresses in the cartilage and local growth front morphology, models that include the epiphysis have shown that it does not affect the overall formation of the bicondylar angle. Future studies will examine how the secondary ossification center affects the local morphology of the growth front.

In this model the growth response immediately followed the stress stimulus. However, in many biological systems there is a lag time in the response, similar to feedback control systems. The tibia-femoral angle (which is different from but related to the bicondylar angle) exhibits a feedback-type response, overshooting the adult value before it stabilizes.^{20,25} Although there are not enough data to determine whether the bicondylar angle has a similar overshoot, incorporation of a lag time in the model would account for the possible overshoot and subsequent correction of certain growth patterns in bone morphogenesis.

Mechanobiological principles may be useful in explaining other morphological features in the paleontological record, particularly those that reflect a change in function or loading conditions. Using mechanobiological principles to predict how stresses affect bone growth may have significant clinical implications as well. For example, in congenital hip displacement the head of the femur develops outside of the acetabular socket. This abnormal loading results in abnormal growth front progression. Similarly, children with cerebral palsy who walk with a crouched gait have abnormal joint loads and subsequently develop bony deformities. Understanding how joint loading affects the formation of these bony deformities may help clinicians treat these conditions before the deformities develop.

The formation of the bicondylar angle in phylogeny is therefore not an intrinsic genetic trait that distinguishes early hominids from apes, but rather a skeletal response to a change in locomotor activity. Appearance of the bicondylar angle in phylogeny reflects developmental mechanics seen in ontogeny and is indicative of bipedal gait. These mechanobiological concepts provide a strong basis for future study of bone growth in response to mechanical loading and can be incorporated into our understanding of overall bone development and skeletal morphogenesis.

Acknowledgments: This work was supported by a National Science Foundation Fellowship, a Stanford Graduate Fellowship, and the Palo Alto VA RR&D Center. The authors thank Gary Beaupré, Allison Arnold, Deanna Asakawa, Silvia Blemker, Scott and Ryan Yerby, Gary Gold, and Tim Weaver for their contributions, comments, and suggestions.

References

1. Aiello, L. and Dean, C. An Introduction to Human Evolutionary Anatomy. London: Academic; 1990.
2. Carter, D. R., Mikic, B., and Padian, K. Epigenetic mechanical factors in the evolution of long bone epiphyses. *Zool J Linnean Soc* 123:163–178; 1998.
3. Carter, D. R., Orr, T. E., Fyhrie, D. P., and Schurman, D. J. Influences of mechanical stress on prenatal and postnatal skeletal development. *Clin Orthopaed* 219:237–250; 1987.
4. Carter, D. R., Rappoport, D. J., Fyhrie, D. P., and Schurman, D. J. Relation of coxarthrosis to stresses and morphogenesis. A finite element analysis. *Acta Orthopaed Scand* 58:611–619; 1987.
5. Carter, D. R. and Wong, M. The role of mechanical loading histories in the development of diarthrodial joints. *J Orthop Res* 6:804–816; 1988.

6. Carter, D. R. and Wong, M. Mechanical stresses in joint morphogenesis and maintenance. In: Mow, V. C., Ratcliffe, A., and Woo, S. L. Y., Eds. *Biomechanics of Diarthroidal Joints*. New York: Springer; 1990; 155–174.
7. Frost, H. M. Skeletal structural adaptations to mechanical usage (SATMU): 3. The hyaline cartilage modeling problem. *Anat Rec* 226:423–432; 1990.
8. Hall, B. K. and Herring, S. W. Paralysis and growth of the musculoskeletal system in the embryonic chick. *J Morphol* 206:45–56; 1990.
9. Harrington, I. J. A bioengineering analysis of force actions at the knee in normal and pathological gait. *Biomed Eng* 11:167–172; 1976.
10. Heegaard, J. H., Beaupre, G. S., and Carter, D. R. Mechanically modulated cartilage growth may regulate joint surface morphogenesis. *J Orthop Res* 17:509–517; 1999.
11. Heiple, K. G. and Lovejoy, C. O. The distal femoral anatomy of Australopithecus. *Am J Phys Anthropol* 35:75–84; 1971.
12. Hurwitz, D. E., Sumner, D. R., Andriacchi, T. P., and Sugar, D. A. Dynamic knee loads during gait predict proximal tibial bone distribution. *J Biomech* 31:423–430; 1998.
13. Johnson, F., Leitz, S., and Waugh, W. The distribution of load across the knee. A comparison of static and dynamic measurements. *J Bone Jt Surg [Br]* 62:346–349; 1980.
14. Johnson, F., Scarrow, P., and Waugh, W. Assessment of loads in the knee joint. *Med Biol Eng Comput* 19:237–243; 1981.
15. Kember, N. F. and Sissons, H. A. Quantitative histology of the human growth plate. *J Bone Jt Surg [Br]* 58-B:426–435; 1976.
16. Klein, R. G. *The Human Career: Human Biological and Cultural Origins*. Chicago, IL: University of Chicago; 1999.
17. Laplaza, F. J., Root, L., Tassanawipas, A., and Glasser, D. B. Femoral torsion and neck-shaft angles in cerebral palsy. *J Pediatr Orthop* 13:192–139; 1993.
18. Leakey, M. G., Feibel, C. S., McDougall, I., and Walker, A. New four-million-year-old hominid species from Kanapoi and Allia Bay, Kenya. *Nature* 376:565–571; 1995.
19. Leakey, M. G., Feibel, C. S., McDougall, I., Ward, C., and Walker, A. New specimens and confirmation of an early age for Australopithecus anamensis. *Nature* 393:62–66; 1998.
20. MacMahon, E. B., Carmines, D. V., and Irani, R. N. Physiologic bowing in children: an analysis of the pendulum mechanism. *J Pediatr Orthop B* 4:100–105; 1995.
21. Morrison, J. Bioengineering analysis of force actions transmitted by the knee joint. *Bio-Med Eng* 3:164–170; 1968.
22. Parsons, F. G. The characters of the English thigh bone. *J Anat Physiol* 48:238–267; 1914.
23. Pauwels, F. *Biomechanics of the Locomotor Apparatus*. Berlin: Springer; 1980.
24. Preuschoft, H. and Tardieu, C. Biomechanical reasons for the divergent morphology of the knee joint and the distal epiphyseal suture in hominoids. *Folia Primatol* 66:82–92; 1996.
25. Salenius, P. and Vankka, E. The development of the tibiofemoral angle in children. *J Bone Jt Surg [Am]* 57:259–261; 1975.
26. Schipplein, O. D. and Andriacchi, T. P. Interaction between active and passive knee stabilizers during level walking. *J Orthop Res* 9:113–119; 1991.
27. Stevens, S. *Mechanical Regulation of Articular Cartilage Development, Maintenance, and Degradation*. Stanford, CA: Stanford University; 1997.
28. Stevens, S. S., Beaupre, G. S., and Carter, D. R. Computer model of endochondral growth and ossification in long bones: Biological and mechanobiological influences. *J Orthop Res* 17:646–653; 1999.
29. Tardieu, C. and Damsin, J. P. Evolution of the angle of obliquity of the femoral diaphysis during growth — correlations. *Surg Radiol Anat* 19:91–97; 1997.
30. Tardieu, C. and Preuschoft, H. Ontogeny of the knee joint in humans, great apes and fossil hominids: Pelvi-femoral relationships during postnatal growth in humans. *Folia Primatol* 66:68–81; 1996.
31. Tardieu, C. and Trinkaus, E. Early ontogeny of the human femoral bicondylar angle. *Am J Phys Anthropol* 95:183–195; 1994.
32. Trueta, J. *Studies of the Development and Decay of the Human Frame*. Philadelphia: Saunders; 1968.
33. Wong, M. and Carter, D. R. Mechanical stress and morphogenetic endochondral ossification of the sternum. *J Bone Jt Surg* 70-A:992–1000; 1988.
34. Wong, M. and Carter, D. R. A theoretical model of endochondral ossification and bone architectural construction in long bone ontogeny. *Anat Embryol* 181:523–532; 1990.

Date Received: November 16, 2001

Date Revised: January 22, 2002

Date Accepted: January 23, 2002